IJBPAS, November, Special Issue, 2021, 10(11): 432-441
ISSN: 2277–4998

International Journal of Biology, Pharmacy and Allied Sciences (IJBPAS)
'A Bridge Between Laboratory and Reader'

www.ijbpas.com

THE BIO STANDARD AND DYNAMIC STABILITY MODELS TO ENHANCE THE RESULTS OF AN INCOMING RC COMMUNICATIONS TOWER

RUPINDER SINGH[1*], MUDE SREENIVASULU[2], VANITHA ALAGESAN[3], JAYAPRATHA T[4], MUSTAFA KAMAL[5] AND SADDAM HUSSAIN[6]

1: Associate Professor in Computer Applications at CBSA, Chandigarh Group Of Colleges Landran Sector 112, Landran, Sahibzada Ajit Singh Nagar, Punjab, India

2: Associate Professor in Electronics and Communication Engineering at Samskruti college of Engineering and Technology, Ghatkesar, Hyderabad, India

3: Assistant Professor, Department of MCA, Sona College of Technology, Salem, Tamilnadu, India

4: Assistant Professor in Computer Science and Engineering at Sri Eshwar College of Engineering, Coimbatore, India

5: Department of Basic Sciences, College of Science and Theoretical Studies, Saudi Electronic University, Dammam, 32256, Kingdom of Saudi Arabia

6: PhD scholar in Civil and Architecture Engineering at Kyushu institute of technology, Kitakyushu Fukuoka, Japan

***Corresponding Author: Rupinder Singh; E Mail: rupinder.3573@cgc.edu.in**

Received 20th July 2021; Revised 22nd Aug. 2021; Accepted 30th Sept. 2021; Available online 1st Nov. 2021

https://doi.org/10.31032/IJBPAS/2021/10.11.1038

ABSTRACT

Another of the goals for the research is to offer a new dynamics paradigm based on real-world data with NBR-6123-87 that can be employed to undertake a complex dynamics evaluation of small structures subjected to wind pressure. The steady reaction, which is provided by the average wind velocity, is first calculated. Throughout this portion on the problem, they

apply time notion is optimal flexibility for expressing substances physiologically reactions employing the P-Delta method, which displays mathematically change. Employing the interrupted dynamics modelling given by NBR-6123-87 plus the eventual stiffness determined employing a P-Delta theory, analyze aircraft dynamics reaction offered alongside its changing velocity. Standard stability or dynamical models are used to establish the results of an incoming RC telecommunications tower.

Keywords: RC communications; Bio standard; regular dynamic modeling; Stability

INTRODUCTION

These equations given by Brazilian code NBR-6123-87 for performing a dynamical evaluation for constructions susceptible to windy loads include quadratic dynamical systems **[1]**. Conventional theories would cannot accurately capture that performance for RC buildings when the practical elasticity varies constantly owing to irregular substance performance and the degree of power. The computing of bridge qualities, and hence deflections and structural pressures, in slender RC constructions submitted to shear force, is a challenging problem since bridge characteristics vary as the lots and lots fluctuate over time **[2-4]**. What hardness do we take into account? Overall average windy velocity & both drifting air velocity are average 2 elements that makeup airspeed. Thus stationary weights of thus superstructure are affected by mean velocity, whereas dynamical overloading is affected by drifting breeze velocities **[5]**. The simulations provided by NBR-6123-87 are quadratic dynamical equations, which assume a continuous elasticity over the duration, which does not occur in actuality.

IJBPAS, November, Special Issue, 2021, 10(11): 432-441
ISSN: 2277–4998

International Journal of Biology, Pharmacy and Allied Sciences (IJBPAS)
'A Bridge Between Laboratory and Reader'
www.ijbpas.com

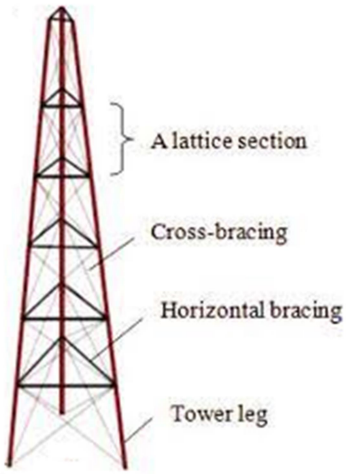

Figure 1: Typical Radio Controlled Telecommunications Tower

These scientists examine a constructed 40 m RC communications mast **(Figure 1)**, which is comparable to those constructed in Brazil's Minas Gerais & Part of public Santos regions. The scientists examine potential polynomial response for the impacts of average wind velocity on structural. A P-Delta influence upon overall architecture would be addressed during the next stage **[6]**. Their maximum tension in each repetition is provided by **[7]**. Following this approach of convergence, we begin computing the dynamical impacts of the breeze as determined from the floated airspeed. This material, according to the researchers, rotates around an optimum point. This is the point determined by the P-Delta product's latest repetition. Both spontaneous patterns and frequency for oscillation were next calculated using the presented excellent determined by the P-Delta product's final cycle. The dynamic analysis may be performed by NBR-6123-87 **[8]** after the intrinsic shape or frequency is determined. The structural performance is determined by adding the static (supplied by both P-Delta technique with curves) and dynamical (supplied using continuous dynamical models of NBR-6123-87) elements.

Linear static analysis

According to NBR-6123-87 **[10]**, V0 is the wind speeds estimated every 3 seconds

at the height above ten centimeters below the surface, over a flat landscape with no irregularity, and with a 50-year repetition. R_1 is the topographical element, whereas R_2, which is functional, determines overall landscape hardness.

$$R_2 = yE_s\left(\frac{c}{5}\right)^q \quad (1)$$

Where y, q, and E_s are the factors, c represents the height

$$U_i = U_0 \,.R_1\,.R_2.R_3, \quad p = 0.613.U_i{}^2 \quad (2)$$

$$Factor = p.Z_x.\ Area \quad (3)$$

Where Z_x represents the coefficient

Linear dynamic analysis (LDA)

For NBR-6123-87, kth degree of freedom, the total load A_k Overall total both this average drifting loads due to straight breeze is defined by

$$A_k = \bar{A}_k + \hat{A}_k \quad (4)$$

Where the mean load $\bar{A}_k$ is

$$\bar{A}_k = \bar{p}_0 y^2 Z_k X_k \left(\frac{c_k}{c_s}\right)^{2q} \quad (5)$$

Where $\bar{p}_0 = 0.613$

$$\bar{u}_q = 0.69u_o R_1 R_3 \quad (6)$$

The floating component $\bar{A}_k$ is given by

$$\bar{A}_k = E_G \alpha_k \beta_k \quad (7)$$

Where

$$\alpha_k = \frac{n_k}{n_0}, E_G = \bar{p}_0 y^2 X_0 \frac{\sum_{j=1}^{m} \alpha_j \beta_j}{\sum_{j=1}^{m} \gamma_j {\beta_j}^2} \quad (8)$$

$$J_{total} = J_z + J_r\,, where\, J_r = J_r \frac{F_r}{F_z} - 1 \quad (9)$$

J_{total} becoming, including both, this same metal viscoelastic strength but also ng, the tangent flexural tensile of cement, its cumulative shear wall stainless location facility of gravity linked to the configuration spectrum, the corporatized translational sheet metal region point in time of rigidity, its overall bridge area juncture of resistance, and the distinctive contractile reaction in MPa at 28 days cement **[11]**. We use the bridge center of gravity for its overall modulus because this approach is founded on quadratic model equations.

$$J = J_{total} \quad (10)$$

of each segment to determine this building's stress state That presumption may be warranted since, inside a dynamic limit f*framework, any bridge damages may be

taken into account, therefore the hardness to be evaluated would equal the entire rigidity.

$$\hat{P} = \left[\sum_{i=1}^{s} \hat{P}_j^{\,2}\right] \quad (11)$$

And

$$B_j = \frac{1}{3} A_j \quad (12)$$

As said before, there were two types of tensions connected to blustery acceleration: steady tensions caused by breeze rates and loads applied on wandering rapidity. Specially developed throughput limits were considered known as the preliminary responses from certain formulae. At this stage, we assume that the construction is vulnerable to P-Delta phenomena with multiple dynamical pressures. When determining the statistical distances (i(j)) at the ith nodes during a jth repeating using this same P-Delta method, such providing is considered under deliberation. In contrary to whatever was accomplished using the subsequent formulas to predict the angular velocity just between the ith cluster or the jth iteration using such P-Delta methodology:

$$J_{j(k)} = J_{FGj(k)} = v_{j(k)} J_{total} \quad (13)$$

$$\Delta \bar{N}_{ij} = \Delta M_{ij}\left(\bar{\mu}_{ij} - \bar{\mu}_{i(j-1)}\right) \quad (14)$$

Those 2nd batch dynamic external loads are the ultimate findings derived using this formula. We estimate the patterns and harmonics of the building's oscillation using the elasticity acquired in the completion of the P-Delta technique, and so complete the dynamical assessment. We assumed that the architecture removes the P-Delta product's stability location.

Numerical Analysis

This construction under consideration is a 40-meter-long, 60-centimeter-diameter RC communications mast. The construction is a cylinder, having around the bridge. Since overall thicknesses or iron surface of this superstructure increase throughout the axis, the characteristics alter. The limestone employed in the construction of the building has unique durability (f_{ck}) after 28 days, equivalent to 45 MPa, which corresponds with, E_{csec} = 41.4GPa. The building's elastic stiffness is taken into account E = E_{csec}. The masonry is 25 millimeters thick. f_{cd} = 45/1.3MPa was its cement designing resistant. Its metal employed in the construction of the construction has a f_{yd} = 500/1.15MPa (iron designer tension). E_s = 210GPa. The structure is made up of 40 parts, each approximately 1 meter in diameter. These features are shown in **Table 1**. For **Table 1**, we used any of the required

annotations: Component denotes the model length of individual networks in a minimal volumetric approaches (FEM) application. The level of elevation about the floor level is referred to as elevation. Øext is the cross-exterior segment's width; The diameter of the pass is broad; The node mass (crammed bulk) is M. The bridge region is referred to as a whole. nb is the number of longitudinal columns in the reinforcing cement portion; b is the width of horizontal columns; Ic is the round shield's length of gravity; Ic is the circled shield's quantity of resistance; Ic is the circled wall's period of complacency; Ic is the circular ring's occasion of inertia The entire lengthwise steel area is the same. The size of the sphere that runs across the centerline of the bars is Rb. It is the metal city's overall moment of tension. I total is the reinforcement polymer cross-total section's homogeneous moment of inertia, and Is/I total = ws is the reduced delimitation benefit for w at for every segment.

Table 1: Structure of Properties

Node	Ht.	θ	Thick	M	A	Lc	Nb	θb	As	RB	ls	I	Is/I
1	40	50	15	802	1521	500417	20	13	25	27	8643	535650	7
2	39	50	15	420	1521	500417	20	13	25	27	8643	535650	7
3	38	50	15	420	1521	500417	20	13	25	27	8643	535650	7
4	37	50	15	420	1521	500417	20	13	25	27	8643	535650	7
5	36	50	15	420	1521	500417	20	13	25	27	8643	535650	7
6	35	50	14	420	1521	500417	20	13	25	27	8643	535650	7
7	34	50	14	420	1963	576678	20	13	25	27	8643	535650	7
8	33	50	14	520	1963	560211	20	13	25	26	10483	611911	7
9	32	50	14	520	1850	540542	15	16	30	26	10483	611911	7
10	31	50	14	520	1850	537582	15	16	30	26	10483	611911	7
11	30	50	12	520	1731	576678	15	16	30	26	10483	611911	8
12	29	50	12	520	1731	560211	15	16	30	26	10483	583275	8
13	28	50	12	469	1716	540542	15	16	30	26	10483	583275	9
14	27	50	12	469	1716	576678	15	16	30	26	13977	583275	9
15	26	50	12	469	1716	560211	15	20	32	26	13977	580585	9
16	25	50	10	533	1716	540542	16	20	32	26	16136	580585	9
17	24	50	10	599	1716	576678	17	20	34	26	17212	583434	10
18	23	50	10	520	1921	560211	17	20	36	26	17212	583434	10
19	22	50	10	531	2238	540542	18	20	38	26	18288	649664	10
20	21	50	10	531	2238	537582	18	20	410	26	18288	649664	12

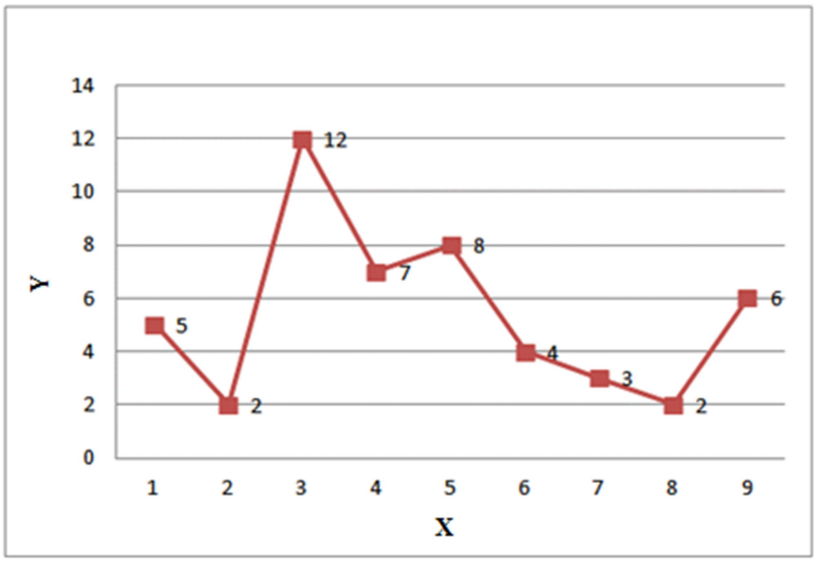

Figure 2: Adopted effective stiffness

We take into account the fundamental air velocity of *V*0 = 35m/s, This topography component is S1 = 1 because this statistical variable was S3 = 1.1. Use topographic harshness grade IV, type B, generates S2(b; p; Fr), where that statistical component becomes S3 =1.1 Hence loading on an area A is F = q, as previously mentioned. ·*Ca* ·*A*, where *Ca* is the parameter of aerodynamics Staircase with generally prorope, a podium with antennae supporters, night signature lights, security over electrostatic discharges mechanism, and deployed antennae are among the technology put on the tower. *A* or *Ca* have enormous quantities., 0 ≤ *z* ≤40m, *A* = 0.6m2/m, and *Ca* = 0.6; catwalks, 0 ≤ *z* ≤40m, *A* = 0.05m2/m and *Ca* = 2; cables, 0 ≤ *z* ≤40m,*A* = 0.15m2/m, and *Ca* = 1.2; Assistance for the base and antennae, *z* = 40m, *A* = 1m2, and *Ca*= 2; antennas, *z* = 40m, *A* = 3m2, and *Ca* = 1. Overall nodes masses (M) and region for the studied configuration are shown in **Table 2**. They can use the following calculations **Figure 2** to calculate average enhancement coefficient:

$$v = -1.5a^3 + 3.3a^2 - 2.5a + 1.1 \quad (15)$$

It's worth noting that the highest number is 1.0 and the data points fluctuate. Regardless of the protection factors used within substances and the designing processes, x figures are frequently seen during testing constructions. = *Mk*/*Mu* ≥1.0. That greatest quantity predicted by xofa 30m construction examined by **[12]** was 1.33, whereas, for another comparable 40m structures, the greatest was x= 1.53.

estimate the inherent patterns or speeds on oscillation using initial combined mass (M)

from **Table 3**, the total homogenous moments of gravity using our LDA modeling, plus actual functional moments of rigidity of the last repetition of the P-Delta technique for the NDA **(Figure 3)**. Harmonic vibrations in the regressive paradigm are less than in the LSA approach. The amplifier index ξ LDA readings were provided through 2.35, while NDA data were provided through 2.65 **[13]**.

Table 3: Homogenous moments of gravity using LDA in 4 levels from Mode

Natural Vibration Modes	Mode 1	Mode 2	Mode 3	Mode 4
Linear Frequency Model	0.13	0.74	2.02	3.38
Nonlinear frequency model	0.08	0.56	1.21	2.65

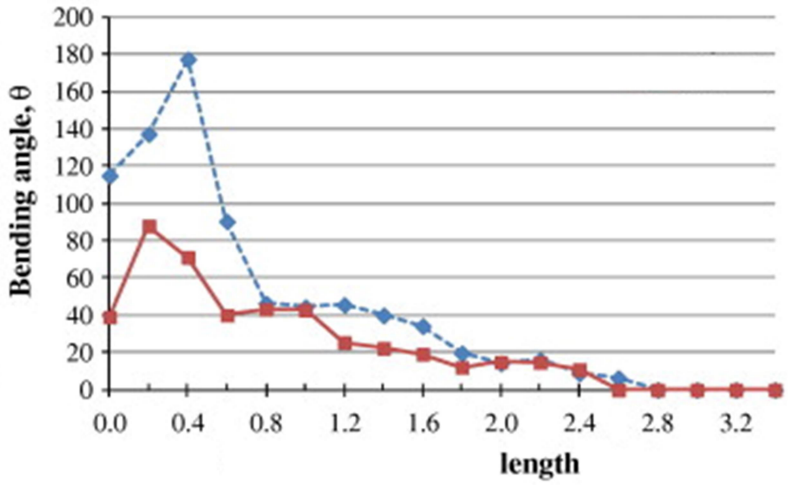

Figure 3: Moments of Bending

Figure 3 shows the bending moment estimates achieved in the scenarios studied. These relevant stretching energies are shown in that diagram: *M*lsa (LSA), *M*lda(LDA), *M*nda (NDA), *M*d (design bending moment), and *M*t (bending moment applied in tests). The LDA displayed folding stress readings that were 1.3 times those of the LSA, while the NDA displayed readings that were 1.5 times those of the LSA. LSA provides 1.4 double the development seconds, whereas LDA provides 1.1 times the innovation occasions. By examining the findings, we can infer that the designer twisting tension is adequate with LDA but not with NDA. Another significant result is the bridge's good performance in terms of the hazard parameter nearing a breakdown. The construction was able to withstand a load of 1.53 times its intended stress. This is owing to the protection equations assigned to elastic modulus, as previously indicated. Test outcomes demonstrate that the construction withstands the bends forces specified by

NDA successfully. Another essential factor to evaluate is the concrete's flexibility stiffness. In this study, we used E = 41.4GPa, which was calculated using NBR-6118-78. Such a number is greater than those standards determined in testing, whose are approximately 21GPa, and larger than even the 31.9GPa with its integrated stonework given either by revolutionary NBR-6118-03 version of the same technology. These findings were similar whether we calculate a certain variables w1(x) using a specific stiffness component of marbles E1 and subsequently resolve very problem with a second quantity E2. w has a unique meaning. $w2(x) = E1w1/E2$, To put it another way, its amount $E1w1 = E2w2 = Eiwi$ At varied quantities of E used, is a consistent.

CONCLUSIONS

Leveraging NBR-6123-discrete 87's multimodal assessment, we provide a regression dynamics architecture based on experimentation knowledge in these studies. The mechanical variability was represented using this improvement approach, while the morphological variability was computed using the P-Delta approach. To express their overall elasticity, we used a cubic polynomial. With every repetition of using the P-Delta technique, we calculated the functional stiffening as a proportion of the strain value. The spontaneous harmonics & patterns for oscillation were computed using both functional moduli achieved in the last round of the P-Delta technique. We assumed that the architecture removes at the P-Delta product's stability location. Lastly, the total of quadratic static and dynamic strengths was calculated. Overall numbers produced from the NDA were determined through testing LSA and the LDA. The LDA displayed twisting strain levels that were 1.3 times these of the LSA, whilst NDA displayed readings that were 1.5 twice these of its LSA. The LSA's development seconds are 1.4 times these of the LDA, while the LDA's creative experiences are 1.1 twice these of the LSA. The designer twisting tension is adequate with the LDA and unsatisfactory with the NDA, researchers determined. Experimental outcomes demonstrate that the construction "in actuality" sustains the bends forces specified by the NDA adequately.

REFERENCES

[1] Alshurafa S, Alhayek H, Polyzois D. Dynamic characteristics of an 8.6 m lightweight FRP tower supporting mass on its top. Marine Structures. 2021 Sep 1; 79: 103052.

[2] Sobrinho CW. Utilização de divisóriasinternas de edifíciose-malvenaria de blocos de gesso-

foconasustentabilidade. Construção, 2018, FEUP, Porto-PT (http://www. itep. br/images/img_noticias/pdf/artigo-principal-carlos. pdf). 2018.

[3] Tak N, Pal A, Choudhary M. A Review on Analysis of Tower on Building with Sloping Ground. International Journal of Advanced Engineering Research and Science. 2020; 7(2): 84-7.

[4] Gómez MA, Díaz-Segura EG, Vielma JC. Nonlinear numerical assessment of the seismic response of hillside RC buildings. Earthquake Engineering and Engineering Vibration. 2021 Apr; 20(2): 423-40.

[5] Asassfeh JA, AlTarawneh M, Samson F. Integrative Model for Quantitative Evaluation of Selection Telecommunication Tower Site. Telkomnika. 2018 Jun 1; 16(3): 1158-64.

[6] Khan S, Jamle S. Use of Shear Wall Member at Corners to Enhance the Stability Using Different Grades: An Immense Review. International Journal of Advanced Engineering Research and Science, (ISSN: 2456-1908 (O), 2349-6495 (P)). 2020; 7(5): 396-400.

[7] da Silva MA, Brasil RM. The non-linear dynamic analysis of RC telecommunication towers considering the effective stiffness.

[8] Prajapati MK, Jamle S. Strength irregularities in the multistoried building using base isolation and damper in high Seismic zone: A theoretical Review. International Journal of Advanced Engineering Research and Science. 2020: 2456-1908.

[9] Paiva F, Barros R, Henriques J, Cunha T, Feyfant P. Dynamic Survey of a Telecommunication Tower by Interferometric Radar Technique. Portuguese Conference on Automatic Control 2020 Jul 1 (pp. 773-782). Springer, Cham.

[10] Depina I, Divić V, Munjiza A, Peroš B. Performance-based wind engineering assessment of critical telecommunication infrastructure subjected to bora wind. Engineering Structures. 2021 Jun 1; 236: 112083.

[11] Latchoumi, T. P., Reddy, M. S., & Balamurugan, K. (2020). Applied Machine Learning Predictive Analytics to SQL Injection Attack Detection and Prevention. *European*

Journal of Molecular & Clinical Medicine, *7*(02), 2020.

[12] Pieraccini M, Fratini M, Parrini F, Pinelli G, Atzeni C. Dynamic survey of architectural heritage by high-speed microwave interferometry. IEEE Geoscience and Remote Sensing Letters. 2005 Jan 17; 2(1): 28-30.

[13] Atzeni C, Bicci A, Dei D, Fratini M, Pieraccini M. Remote survey of the leaning tower of Pisa by interferometric sensing. IEEE Geoscience and Remote Sensing Letters. 2009 Oct 20; 7(1): 185-9.